J. Fluid Mech. (1978), *vol.* 85, *part* 2, *pp.* 209–232
Printed in Great Britain

The rheology of suspensions of charged rigid spheres

By WILLIAM B. RUSSEL

Department of Chemical Engineering, Princeton University, Princeton, New Jersey 08540

(Received 21 July 1976)

The rheology of particulate dispersions which are strongly influenced by particular types of non-hydrodynamic forces is analysed within the framework of suspension mechanics. Interactions between particles in a homogeneous shear flow without inertia are governed by viscous, electrostatic, London–van der Waals and Brownian forces. The balance among these provides the fluid with a microstructure described quantitatively at dilute concentrations by a pair distribution function and qualitatively by a characteristic interaction length. The bulk rheology follows from the microstructural variables through suitable averaging.

In dilute electrostatically stabilized suspensions of small rigid spheres for which London–van der Waals attractions and hydrodynamic interactions can be ignored, the theory predicts a Newtonian low-shear limit. The analytic expression for the viscosity contains a ϕ^2-coefficient which can be quite large and agrees well with experimental data. At higher flow strengths a scale analysis of the pair conservation equation indicates a shear- and strain-thinning rheology, representing a breakdown of the fluid microstructure. Without flow the interaction length attains a maximum determined by the balance between Brownian motion and electrostatic repulsion. A weak shear merely perturbs this balance but generates stresses proportional to the fifth power of the length. With increasing shear rate this length and consequently the shear viscosity are reduced until viscous interactions completely dominate. Asymptotic solutions for an intermediate regime in which Brownian motion and hydrodynamic interactions are both negligible reveal power-law extensional and shear viscosities with non-zero normal stresses.

1. Introduction

Suspensions of micron or submicron particles in Newtonian fluids are well known for their complex rheology and its sensitivity to their electrochemical state. For example, Freundlich & Jones (1936) had difficulty discriminating between systems for which the shear viscosity increases with increasing rate of strain (shear-thickening) and those for which it decreases (shear-thinning) solely on the basis of particle size, shape and concentration and solvent type. In retrospect we can attribute this failure to the fact that these parameters do not characterize all the important forces.

Fryling (1963) demonstrated the critical role of electrical forces by transforming a low-viscosity suspension of $\sim 0{\cdot}1\ \mu$m polymer latex spheres into a gel by removing the free electrolyte which shields (or neutralizes) surface charges. More recent experiments on similar spheres in a variety of solvents have revealed several different steady-state viscosity–shear-rate relationships. Krieger (1972) and Krieger & Eguiluz (1976) obtained monotonically decreasing viscosities with a constant high-shear asymptote,

but both finite (Newtonian) and apparently infinite low-shear limits. On the other hand, Hoffman (1972, 1974) observed shear-thinning at low shear rates followed by a continuous, or sometimes discontinuous, increase in viscosity. At still higher shear rates the viscosity steadily decreased again. These phenomena depended strongly on the volume fraction of spheres, their surface charge and the ionic strength of the solvent.

These and other experiments on model systems have successfully correlated some rheological characteristics with microstructural parameters (Jeffrey & Acrivos 1976). The relevant non-hydrodynamic forces appear to be Brownian motion, electrostatic repulsions and London–van der Waals attractions. Quantitative predictions of bulk rheology have been lacking, however. Before proceeding in this direction, we must recognize some of the unique characteristics of suspensions of charged colloidal particles.

Solid particles dispersed in a fluid are thermodynamically unstable since aggregation lowers their free energy. The dispersion can be preserved, however, if the rate of flocculation due to London–van der Waals attractions is sufficiently reduced by electrostatic repulsion between like surface charges. The classical Derjaguin–Landau–Verwey–Overbeek theory (Verwey & Overbeek 1948) combines these interparticle forces with Brownian motion to quantitatively predict stability criteria and flocculation rates for such dilute electrostatically stabilized suspensions of spheres. Recently Spielman (1970) and Honig, Roebersen & Wiersema (1971) have modified the theory to account correctly for viscous interactions at small separations.

When velocity or electric fields are applied to systems of charged particles so-called electrokinetic phenomena arise. These owe their unusual character to the interaction among viscous, Brownian and electrical forces in the interfacial region, where counterions attracted from the bulk fluid form a diffuse ion cloud which shields the surface charge. The extent of this 'electrical double layer' is characterized by the Debye length $1/\kappa$, which is generally $0{\cdot}1\ \mu$m or smaller in aqueous systems. Thus electrostatic forces will be significant only for micron or submicron particles unless the concentrations are high enough for the characteristic separation to be submicron. At these length scales inertia is negligible even for quite strong flows.

These phenomena can be described mathematically by first adding an electrostatic body-force term to the Stokes equations to obtain

$$-\nabla p+\mu_0\nabla^2\mathbf{u}=\rho\nabla\psi,\quad \nabla\cdot\mathbf{u}=0. \tag{1}$$

Here $\mathbf{u}$ is the fluid velocity, p the pressure, μ_0 the viscosity, ψ the electrostatic potential and ρ the charge density. The last is related to the number densities n^k of the individual ions through the valences z^k by

$$\rho=e\sum_k z^k n^k, \tag{2}$$

where e is the electronic charge. The ion conservation equations which determine the n^k, i.e.

$$\frac{\partial n^k}{\partial t}+\mathbf{u}\cdot\nabla n^k=\omega^k kT\left\{\nabla^2 n^k+\frac{ez^k}{kT}\nabla\cdot n^k\nabla\psi\right\}, \tag{3}$$

can be derived from the convective, diffusive and conductive fluxes for point charges. Here ω^k is the ionic mobility, k Boltzmann's constant and T the temperature. Finally, Poisson's equation

$$\nabla^2\psi=(-4\pi/\epsilon)\rho, \tag{4}$$

with ϵ the dielectric constant of the fluid, completes the set.

Without flow or an external electric field the conservation equations integrate to the Boltzmann distributions

$$n^k = n_0^k \exp(-ez^k\psi/kT),$$

where $n^k \to n_0^k$ and $\psi \to 0$ in the bulk fluid. This represents an equilibrium between electrostatic attraction and thermal motion and leads to the Poisson–Boltzmann equation

$$\nabla^2\psi = -\frac{4\pi e}{\epsilon}\sum_k z^k n_0^k \exp\left(-\frac{ez^k\psi}{kT}\right), \tag{5}$$

which describes the potential within an equilibrium double layer. For a sufficiently small surface charge density $ez^k\psi/kT$ will be small everywhere and the exponentials can be linearized to obtain the Debye–Huckel approximation

$$\nabla^2\psi = \kappa^2\psi, \tag{6}$$

where

$$\kappa^2 = \frac{4\pi e^2}{\epsilon kT}\sum_k z^{k2} n_0^k.$$

For a flat double layer with surface potential ψ_0

$$\psi = \psi_0 e^{-\kappa x}, \tag{7}$$

demonstrating that ψ/ψ_0 falls to $1/e$ at a distance $x = 1/\kappa$ from the surface. Also

$$\int_0^\infty x\rho(x)\,dx \Big/ \int_0^\infty \rho(x)\,dx = 1/\kappa, \tag{8}$$

indicating that the Debye length characterizes the 'centre of charge' of the diffuse ion cloud.

Electrokinetic and electroviscous phenomena entail a disturbance of the equilibrium double layer. For example, any motion of the bulk fluid relative to the interface will convect ions and affect n^k through the second term in (3). In response the electrostatic and Brownian forces attempt to restore equilibrium by moving the ions relative to the fluid, thereby dissipating energy. Booth (1950) solved these equations for uniform straining of magnitude γ around a single sphere of radius a with a small surface charge Q. He obtained the following for the viscosity μ of a suspension of these neutrally buoyant spheres at small volume fractions ϕ:

$$\frac{\mu/\mu_0 - 1}{\frac{5}{2}\phi} = \beta_0 = 1 + Pe^* q^2 Z(a\kappa), \tag{9}$$

where $Pe^* = \epsilon kT/e^2\mu_0\omega^0$, $q = e^2Q/4\pi a\epsilon kT$, $Z(a\kappa)$ = dimensionless function tabulated in his paper and ω^0 = characteristic ionic mobility. Similarly, Booth (1954) derived the extra drag on a sphere translating with velocity u through a quiescent fluid as

$$\text{drag}/6\pi\mu_0 au = \beta_1 = 1 + 4Pe^* q V_3(a\kappa), \tag{10}$$

where $V_3(a\kappa)$ was also tabulated. These results pertain to small ion Péclet numbers

$$Pe = a^2\gamma/\omega^0 kT \quad \text{or} \quad au/\omega^0 kT$$

for which the convection only slightly distorts the equilibrium double layer. β_0 and β_1 are generally close to one. A comprehensive review by Saville (1977) contains a more detailed description of these and other electrokinetic phenomena.

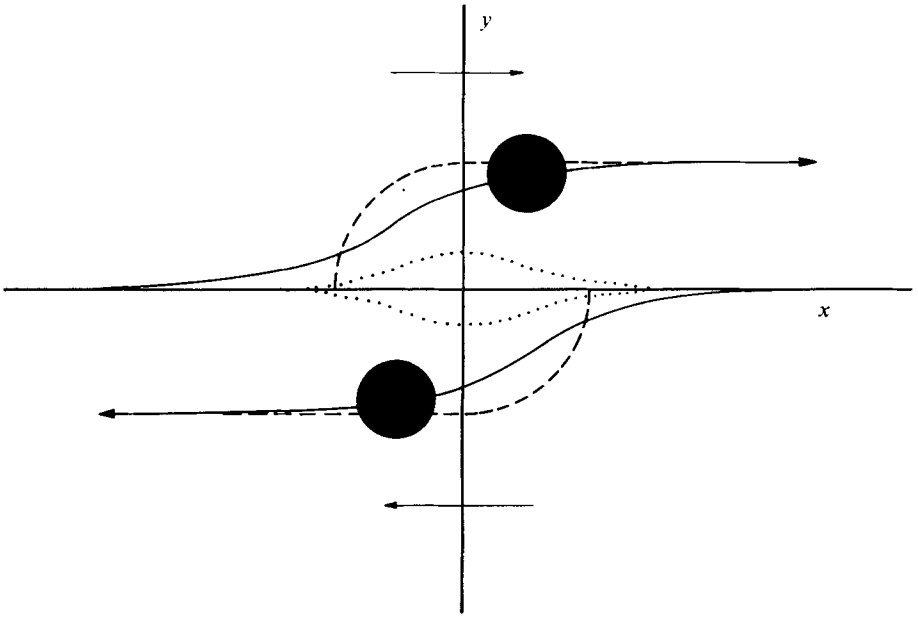

FIGURE 1. Interactions between two spheres in a shear flow. ····, uncharged with hydrodynamic interactions; ——, charged without hydrodynamic interactions; – – –, according to Chan *et al.* (1966).

At higher concentrations electrostatically stabilized colloidal suspensions can be substantially more viscous than suspensions of larger particles because of the interparticle forces. As two charged spheres approach one another in a simple shear flow (figure 1), the electrostatic repulsion forces them across fluid streamlines, dissipating energy. This phenomena, known as the secondary electroviscous effect, was first analysed by Chan, Blachford & Goring (1966). They hypothesized straight upstream and downstream trajectories connected by the arc of a circle along which the electrostatic and viscous forces approximately balance (figure 1). The additional dissipation and, hence, the effective shear viscosity were shown to be proportional to the displacement normal to the undisturbed streamlines. Since viscous forces increase with shear rate while the electrostatic force remains constant, the displacement and the viscosity must decrease with increasing shear rate. Thus the analysis, though crude, qualitatively predicts the observed shear-thinning. Unfortunately, the approach reveals nothing about normal stresses or characteristic time scales. Furthermore, Brownian motion, which dominates the zero-shear limit, was omitted, generating an infinite viscosity contrary to experimental results on dilute suspensions (Stone-Masui & Watillon 1968).

This paper and an earlier one (Russel 1976) begin a full analysis of the bulk rheology of electrostatically stabilized colloidal suspensions. Suspension mechanics provides the framework within which colloidal forces are combined with a proper treatment of the fluid mechanics.

2. Colloidal interactions

The analysis below pertains to monodisperse suspensions of charged rigid spheres surrounded by an electrical double layer whose thickness is characterized by the Debye length $1/\kappa$. For neutrally buoyant colloidal particles the Reynolds number defined in terms of the radius a and the second invariant of the rate of strain γ, i.e. $Re = \rho a^2\gamma/\mu_0$, is small even for strong flows; for example, for 1 μm spheres in water at $\gamma \sim 10^3\,\mathrm{s}^{-1}$, $Re \sim 10^{-3}$. Inertia can therefore be neglected.

Two additional assumptions simplify the analysis. Sufficiently strong electrostatic repulsions prevent close approach of the spheres, allowing both hydrodynamic interactions and molecular attractions to be neglected. Consequently, flocculated suspensions are excluded from the theory. Second, only double layers slightly perturbed from equilibrium will be considered. As demonstrated previously (Russel 1976), this requires both Pe and the electric Hartman number, given by

$$H_e^2 = \epsilon\psi_0^2/4\pi\mu_0\omega_0 kT(a\kappa)^2,$$

to be small. Then (9) and (10) adequately describe the primary electroviscous effect and the drag on an individual sphere. For 0·1–1·0 μm spheres Pe will remain small for shear rates less than $10^3\,\mathrm{s}^{-1}$; H_e^2, however, is $O(1)$ for $\psi_0 \gtrsim 25\,\mathrm{mV}$, so this assumption must eventually be re-examined.

For a study of rheological phenomena which depend on interparticle forces, pair interactions provide the simplest relevant model. The suspension microstructure can then be described statistically by the probability density $P(\mathbf{x}_0+\mathbf{r}|\mathbf{x}_0)$ of finding a second sphere at $\mathbf{x}_0+\mathbf{r}$ given a test sphere at $\mathbf{x}_0$. Since the total number of spheres remains constant in a closed system, a conservation equation for P can be derived from the convective and diffusive fluxes:

$$\partial P/\partial t + \nabla . P\mathbf{u} = \nabla . \mathbf{D} . \nabla P. \tag{11}$$

Here hydrodynamic interactions between the spheres can be included in the relative velocity $\mathbf{u}$ and the relative diffusion tensor $\mathbf{D}$. Explicit forms for these functions can be found in Batchelor & Green (1972) and Batchelor (1975).

Without hydrodynamic interactions the equation reduces to a form originally proposed by Smoluchowski (1917) in his classical work on Brownian and shear-induced flocculation. Then

$$\mathbf{u} = \mathbf{F}_{el}/3\pi\mu_0 a\beta_1 + \nabla\mathbf{u} . \mathbf{r}, \tag{12}$$

where $\mathbf{F}_{el}$ = electrostatic force on each sphere, $\nabla\mathbf{u}$ = bulk velocity gradient, $\mathbf{r}$ = relative position vector and

$$\mathbf{D} = \frac{kT}{3\pi\mu_0 a\beta_1}\boldsymbol{\delta}, \tag{13}$$

which equals the sum of the individual diffusivities.

Although no general electrostatic force law for two charged spheres has been obtained from the nonlinear Poisson–Boltzmann equation (5), two approximations suit our current needs. For small surface potentials ($e\psi_0/kT \ll 1$) and separations $r - 2a$ larger

than $1/\kappa$, the linearized potentials around isolated spheres can be superimposed. Bell, Levine & McCartney (1970) thus determined

$$\mathbf{F}_{el} = \epsilon\psi_0^2 a^2(1+\kappa r)\, r^{-2} e^{-\kappa(r-2a)}. \tag{14}$$

For thin double layers ($a\kappa \gg 1$) and separations larger than $1/\kappa$ but smaller than a, the exact solution for two flat plates can be adapted to spheres. An outer solution, for separations larger than a, of the form (14) completes the force law as (Bell & Peterson 1972)

$$\mathbf{F}_{el} = 8\epsilon \left(\frac{kT}{ez}\right)^2 a\kappa \tanh^2 \frac{ez\psi_0}{4kT}\, e^{-\kappa(r-2a)} \begin{Bmatrix} 1 \text{ for } 1/\kappa \ll r-2a \ll a, \\ 2a/r \text{ for } a \ll r-2a. \end{Bmatrix} \tag{15}$$

Both forces decay exponentially for $\kappa(r-2a) > 1$ owing to the shielding of the surface charge by the counter-ions in the double layer.

Finally, a bulk stress is needed to relate the microstructure characterized by P to macroscopically observable forces. Volume and ensemble averaging techniques developed for suspension mechanics have been discussed by Batchelor (1970). The development depends on the existence of an intermediate length scale chosen much smaller than the macroscopic scale of the flow process but much larger than both the characteristic particle dimension and the mean separation. Then a bulk stress $\boldsymbol{\Sigma}$ satisfying a macroscopic equilibrium equation $\nabla . \boldsymbol{\Sigma} = 0$ can be determined. In the electrostatically dilute limit $\phi^{\frac{1}{3}}/a\kappa \ll 1$, electrostatic forces can be included as

$$\boldsymbol{\Sigma} = -\frac{1}{V}\int_{V-\Sigma V_n} p\boldsymbol{\delta} dV + \mu_0(1+\tfrac{5}{2}\beta_0\phi+\tfrac{5}{2}\beta_0^2\phi^2)(\nabla\mathbf{u}+(\nabla\mathbf{u})^{\mathrm{T}}) + \frac{3\phi}{8\pi a^3}\int \mathbf{r}\mathbf{F}(\mathbf{r})\, P(\mathbf{x}_0+\mathbf{r}|\mathbf{x}_0) d^3\mathbf{r}. \tag{16}$$

(a) (b) (c) (d)

The individual terms are (*a*) the solven tstress, (*b*) the single-particle contribution, (*c*) the far-field, or kinematic, hydrodynamic interaction and (*d*) the interparticle-force contribution. The last three terms comprise the spheres' contribution to the bulk stress if near-field hydrodynamic interactions are ignored. Batchelor & Green (1972) obtained the residual interaction term (*c*) while (*d*) was derived by Russel (1976) from the disturbance due to two well-separated spheres at relative positions $\mathbf{r}$ subject to equal but opposite forces $\mathbf{F}$ and $-\mathbf{F}$. The dipole form of the latter resembles the bulk stress for molecular models with entropic springs connecting spherical beads (Bird, Warner & Evans 1971).

In the next section the above equations are scaled to characterize the rheology qualitatively before results are presented for two limiting cases.

3. Scale analysis of pair interactions

The interaction of two colloidal particles under the influence of Brownian motion, electrostatic repulsion and viscous forces can be characterized by a separation L at which the magnitude of the electrostatic force becomes comparable to those bringing the particles together. The former increases rapidly with further decreases in separation, virtually excluding closer approach and causing the pair density to vary sharply from $O(n)$ outside L to ≈ 0 inside. While one might expect L to vary from $2a$, for negligible repulsion, to infinity, for dominant repulsion, multiparticle interactions will always become significant around the mean separation $2a/\phi^{\frac{1}{3}}$.

With L as the length scale the colloidal and hydrodynamic portions of the particle stress given by terms (d) and (b)–(c) in (16) have magnitudes

$$\left.\begin{aligned} \Sigma^{\text{coll}} &\sim \underset{\substack{\text{dipole}\\ \text{strength}}}{6\pi\mu_0 a L^2\gamma} \times \underset{\substack{\text{volume of}\\ \text{integration}}}{L^3} \times \underset{\substack{\text{pair}\\ \text{probability}}}{n^2} \sim \mu_0\gamma(L/a)^5\phi^2, \\ \Sigma^{\text{hyd}} &\sim \mu_0\gamma\phi(1+\phi). \end{aligned}\right\} \tag{17}$$

Thus with strong repulsive forces L/a will be large and the colloidal contribution to the bulk stress will overwhelm the hydrodynamic contribution. The magnitude of L is estimated below from the pair conservation equation for thick double layers ($a\kappa \ll 1$) with (14) for the electrostatic force while analogous results for thin double layers ($a\kappa \gg 1$) with (15) are described later.

The individual terms in the pair conservation equation are

$$\text{convection} \sim \kappa L\gamma,$$

$$\text{electrostatic} \sim \frac{\epsilon\psi_0^2 a\kappa}{3\pi\mu_0\beta_1}\frac{1+\kappa L}{L^2}e^{2a\kappa}e^{-\kappa L},$$

$$\text{diffusion} \sim \frac{kT\kappa^2}{3\pi\mu_0 a\beta_1},$$

suggesting two dimensionless groups:

$$\alpha = \frac{\epsilon\psi_0^2 a}{kT}a\kappa e^{2a\kappa} \sim \frac{\text{electrostatic force}}{\text{Brownian motion}},$$

$$\Gamma = \frac{3\pi\mu_0 a^3\beta_1}{kT}\frac{\gamma}{(a\kappa)^2} \sim \frac{\text{viscous force}}{\text{Brownian motion}}.$$

For the suspensions considered here, flocculation is prevented by strong electrostatic forces; hence α will be quite large. The magnitude of Γ, however, varies with the rate of strain. From the dimensionless forms of the above terms,

$$\text{convection} \sim \Gamma\kappa L,$$

$$\text{electrostatic} \sim \alpha\frac{1+\kappa L}{(\kappa L)^2}e^{-\kappa L},$$

$$\text{diffusion} \sim 1,$$

we can now determine κL as a function of α and Γ.

For weak flows convection can be neglected to first order, leaving the electrostatic and diffusion terms to balance at

$$L \sim \frac{1}{\kappa}\ln\frac{\alpha}{\ln(\alpha/\ln\alpha)} \equiv \frac{1}{\kappa}\mathscr{L}(\alpha), \quad \text{say.}$$

The bulk stress follows as

$$\Sigma^{\text{coll}} \sim \mu_0\gamma\phi^2[\mathscr{L}(\alpha)/a\kappa]^5,$$

with convection remaining negligible so long as $\Gamma \ll 1/\mathscr{L}(\alpha)$.

Alternatively, for strong flows diffusion plays a minor role and convection must balance the electrostatic force:

$$\frac{\Gamma}{\alpha} \sim \frac{1+\kappa L}{(\kappa L)^3}e^{-\kappa L}. \tag{18}$$

	L	$\Sigma^{(p)}/\mu_0\gamma$
$\Gamma \ll \left(\ln \frac{\alpha}{\ln(\alpha/\ln\alpha)}\right)^{-1}$	$\frac{1}{\kappa}\ln\frac{\alpha}{\ln(\alpha/\ln\alpha)}$	$\phi^2\left\{1+\left[\frac{1}{a\kappa}\ln\left(\frac{\alpha}{\ln(\alpha/\ln\alpha)}\right)\right]^5\right\}$
$\left(\ln\frac{\alpha}{(\ln\alpha)^2}\right)^{-1} \ll \Gamma \ll \alpha$	$\frac{1}{\kappa}\ln\frac{\alpha'}{\{\ln[\alpha'/(\ln\alpha')^2]\}^2}$†	$\phi^2\left\{1+\left[\frac{1}{a\kappa}\ln\left(\frac{\alpha'}{\{\ln[\alpha'/(\ln\alpha')^2]\}^2}\right)^5\right]\right\}$†
$\alpha \ll \Gamma \ll \frac{\alpha}{(a\kappa)^3}$	$\frac{1}{\kappa}\left(\frac{\alpha}{\Gamma}\right)^{\frac{1}{3}}$	$\phi^2\left\{1+\frac{(\alpha/\Gamma)^{\frac{5}{3}}}{(a\kappa)^5}\right\}$
$\frac{\alpha}{(a\kappa)^3} \ll \Gamma$	$2a$	ϕ^2

† $\alpha' \equiv \alpha/\Gamma$.

TABLE 1. Scale analysis for $a\kappa \ll 1$.

Here two asymptotic limits for κL are possible depending on the magnitude of Γ/α. When the flow is still weak compared with the electrostatic force, $\Gamma/\alpha \ll 1$ and the interaction occurs at the outer edge of the double layers, where the repulsion decays exponentially, so that

$$L \sim \frac{1}{\kappa}\ln\frac{\alpha/\Gamma}{\ln\left(\frac{\alpha/\Gamma}{(\ln\alpha/\Gamma)^2}\right)^2} \equiv \frac{1}{\kappa}\mathscr{L}'(\alpha/\Gamma), \quad \text{say,}$$

and

$$\Sigma^{\text{coll}} \sim \mu_0\gamma\phi^2[\mathscr{L}'(\alpha/\Gamma)/a\kappa]^5.$$

Such 'weak' interactions will occur without significant Brownian motion provided that

$$\left(\ln\frac{\alpha}{(\ln\alpha)^2}\right)^{-1} \ll \Gamma \ll \alpha.$$

When Γ becomes larger than α the interaction moves into the inner, or Coulombic, region, for which $\kappa L \ll 1$. Then ionic shielding is negligible, so that (18) yields

$$L \sim \kappa^{-1}(\alpha/\Gamma)^{\frac{1}{3}}$$

and from (17)

$$\Sigma^{\text{coll}} \sim \mu_0\gamma\phi^2(\alpha/\Gamma)^{\frac{5}{3}}/(a\kappa)^5.$$

The colloidal stress will still dominate the hydrodynamic component provided that $\Gamma \ll \alpha/(a\kappa)^3$. Eventually, the increasing flow strength must overcome the repulsive force when $\Gamma \gg \alpha/(a\kappa)^3$, leaving

$$L \sim 2a, \quad \Sigma^{\text{hyd}} + \Sigma^{\text{coll}} \sim \mu_0\gamma\phi(1+\phi).$$

The summary in table 1 illustrates several points. First, an electrostatically stabilized suspension in which pair interactions dominate the rest state, i.e.

$$\frac{\phi^{\frac{1}{3}}}{2a\kappa}\mathscr{L}(\alpha) \ll 1,$$

should have a relative viscosity $\Sigma/\mu_0\gamma$ which is constant for weak flows but decreases with increasing rate of strain. Second, the breakdown of structure producing this

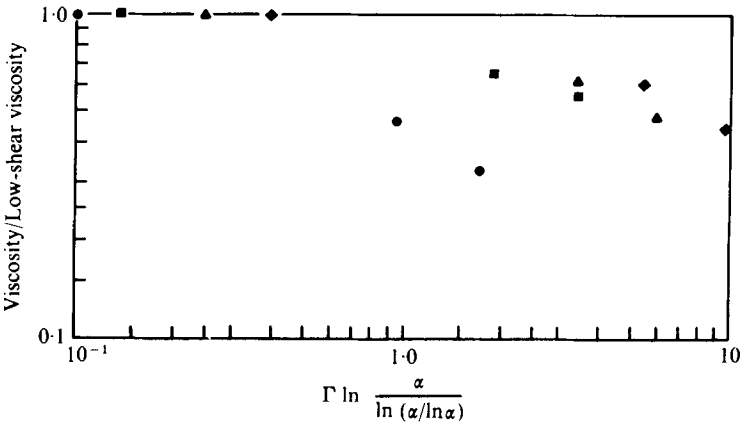

FIGURE 2. Normalized shear-viscosity data of Chan *et al.* (1966) on polymer lattices. ●, $\alpha e^{-4a\kappa} = 0{\cdot}70$; ■, $\alpha e^{-4a\kappa} = 9{\cdot}7$; ▲, $\alpha e^{-4a\kappa} = 35$; ◆, $\alpha e^{-4a\kappa} = 75$.

strain-thinning is governed by two different time scales even for a monodisperse system:

$$\frac{3\pi\mu_0 a^3}{kT}\frac{\beta_1}{(a\kappa)^2} \quad \text{(Brownian)},$$

$$\frac{3\pi\mu_0\beta_1}{\epsilon\psi_0^2\kappa^2}\frac{e^{-2a\kappa}}{a\kappa} \quad \text{(electrostatic)}.$$

For thin double layers ($a\kappa \gg 1$), the appropriate electrostatic force law (15) dictates a modification of the first dimensionless group to

$$\alpha = 16\epsilon\frac{kT}{(ez)^5}a(a\kappa)\,e^{2a\kappa}\tanh^2\frac{ez\psi_0}{4kT}. \tag{19}$$

An analogous scaling argument yields similar results except that the inner region disappears and hydrodynamic interactions become important when

$$\Gamma = O(\alpha e^{-4a\kappa}).$$

The data of Chan *et al.* (1966) plotted *vs.* Γ in figure 2 substantiate the scale analysis. The ordinate is the measured ϕ^2-coefficient normalized by its value at the lowest shear rate. Shear-thinning occurs for $\Gamma < O(1)$ and the second time scale qualitatively explains the spread of the curves for $\Gamma > 1$. Even at $16000\,\mathrm{s}^{-1}$ the electroviscous effect persists at $\sim 20\,\%$ of the low-shear value.

The following sections contain analytic solutions for two of the above cases. First a theory valid for arbitrary $a\kappa$ in the low-shear limit is developed as a matched asymptotic expansion for $\alpha \gg 1$. Here the suspension is isotropic and Newtonian. Then the Coulombic interaction limit demonstrates the non-Newtonian behaviour. Both solutions quantitatively support the preceding scale analysis.

4. Low-shear limit

In the absence of flow, Brownian motion and the interparticle electrostatic repulsion balance to determine a spherically symmetric pair distribution for the spheres which resembles the Boltzmann distribution of ions in the double layer. Introduction of a

weak homogeneous shear flow perturbs this distribution slightly and the resulting unbalanced forces generate bulk stresses. In a previous paper (Russel 1976) both the perturbed distribution and the particle stresses were calculated numerically for $e\psi_0/kT \ll 1$, $a\kappa = O(1)$ and $10^2 \leqslant \alpha \leqslant 10^5$. Analytic solutions have now been obtained for this case as well as for $a\kappa \gg 1$ and arbitrary $e\psi_0/kT$ subject to the same restrictions of strong electrostatic repulsions, i.e. $\alpha \gg 1$, and negligible hydrodynamic interactions.

With the linear-superposition approximation (14), the scaled form of (11) with (12) and (13) is

$$\nabla_R^2 P = \alpha \nabla_R . P \frac{1+R}{R^3} e^{-R} \mathbf{R} + \Gamma(\boldsymbol{\Omega} . \mathbf{R} + \mathbf{E} . \mathbf{R}) . \nabla_R P, \tag{20}$$

where $R = \kappa r$, $\mathbf{R}$ is the dimensionless vector separation, and

$$\boldsymbol{\Omega} = \frac{1}{2} \frac{\nabla \mathbf{u} - (\nabla \mathbf{u})^{\mathrm{T}}}{(\nabla \mathbf{u} : \nabla \mathbf{u})^{\frac{1}{2}}}, \quad \mathbf{E} = \frac{1}{2} \frac{\nabla \mathbf{u} + (\nabla \mathbf{u})^{\mathrm{T}}}{(\nabla \mathbf{u} : \nabla \mathbf{u})^{\frac{1}{2}}} \tag{21}$$

are the dimensionless vorticity and rate-of-strain tensors, respectively. The appropriate boundary conditions are

$$\left.\begin{aligned} \frac{\partial P}{\partial R} = P\left\{\alpha \frac{1+R}{R^2} e^{-R} + \Gamma \frac{\mathbf{R} . \mathbf{E} . \mathbf{R}}{R}\right\} \quad \text{at } R = 2a\kappa, \\ P \to n \quad \text{as} \quad R \to \infty, \end{aligned}\right\} \tag{22}$$

representing a stable suspension with zero rate of flocculation and a spatially homogeneous microstructure with number density n at large separations. Then in the low-shear limit, where $\Gamma \ll 1$, the pair density can be expanded as

$$P = P_0\left\{1 + \Gamma \frac{\mathbf{R} . \mathbf{E} . \mathbf{R}}{R^2} f(R)\right\} + O(\Gamma^2). \tag{23}$$

The equilibrium distribution P_0 follows from (20) with $\Gamma \equiv 0$ as

$$P_0 = n \exp(-\alpha e^{-R}/R).$$

The $O(\Gamma)$ equation

$$\frac{1}{R^2} \frac{d}{dR} R^2 \frac{df}{dR} + \alpha \frac{1+R}{R^2} e^{-R} \frac{df}{dR} - \frac{6f}{R^2} = \alpha \frac{1+R}{R} e^{-R}, \tag{24}$$

with

$$f \to 0 \quad \text{as} \quad R \to \infty,$$

$$df/dR = 2a\kappa \quad \text{at} \quad R = 2a\kappa,$$

determines the radial dependence of the perturbation. The particular solution is

$$f_p = \tfrac{1}{2} R^2,$$

leaving the homogeneous solution to satisfy the boundary conditions

$$\left.\begin{aligned} f_h \to -\tfrac{1}{2} R \quad \text{as} \quad R \to \infty, \\ df_h/dR = 0 \quad \text{at} \quad R = 2a\kappa. \end{aligned}\right\} \tag{25}$$

An exact analytic solution for f_h has not been obtained because of the electrostatic force term

$$\alpha \frac{1+R}{R^2} e^{-R} \frac{df_h}{dR},$$

which ranges from $O(\alpha) \gg 1$ for $R = O(1)$ to exponentially small values as $R \to \infty$. The transition occurs in an $O(1)$ region about

$$R \sim \mathscr{L}(\alpha) = \kappa L_0,$$

producing, for example, the equilibrium pair distribution

$$P_0 \sim \begin{cases} 0 & \text{for} \quad R \ll \kappa L_0, \\ n & \text{for} \quad R \gg \kappa L_0. \end{cases}$$

For $\alpha \gg 1$ we seek instead asymptotic solutions in three regions:

(*a*) inner, $R = O(1)$;

(*b*) intermediate, $\rho = R - \kappa L_0 = O(1)$;

(*c*) outer, $R \gg \kappa L_0$.

Then the electrostatic force dominates the inner region, Brownian motion dominates the outer, and only in the intermediate region must both be considered simultaneously.

In (*a*) the appropriate expansion is

$$f_{\text{inner}} = g_0 + g_1/\alpha + \ldots,$$

which produces

$$\left.\begin{aligned} \frac{1+R}{R^2} e^{-R} \frac{dg_0}{dR} &= 0 \\ dg_0/dR = 0 \quad \text{at} \quad R &= 2a\kappa \end{aligned}\right\} \quad \text{at} \quad O(1), \tag{26}$$

$$\left.\begin{aligned} \frac{1+R}{R^2} e^{-R} \frac{dg_1}{dR} &= 6\frac{g_0}{R^2} - \frac{1}{R^2}\frac{d}{dR} R^2 \frac{dg_0}{dR} \\ dg_1/dR = 0 \quad \text{at} \quad R &= 2a\kappa \end{aligned}\right\} \quad \text{at} \quad O(\alpha^{-1}), \tag{27}$$

with general solutions

$$g_0 = c_0, \quad g_1 = (6c_0/e)\,\mathrm{Ei}\,(1+R) + c_1, \tag{28}$$

where e is the exponential and Ei the exponential integral. Without diffusion the expansion is singular and g_1 cannot satisfy the no-flux condition at $R = 2a\kappa$. An 'inner inner' solution valid for $R \sim 2a\kappa$ would resolve this difficulty and uniquely determine c_1 but is unnecessary since c_1 will not be needed further. For later reference

$$\lim_{R \to \kappa L_0} f_{\text{inner}} = c_0 \left\{ 1 + \frac{6e^{\rho}}{[\ln(\alpha/\ln\alpha)]^2} + O\left(\ln\frac{\alpha}{\ln\alpha}\right)^{-3} \right\}. \tag{29}$$

In the intermediate region (24) transforms to

$$\frac{d^2 f}{d\rho^2} + e^{-\rho}\frac{df}{d\rho} - \frac{6f}{[\ln(\alpha/\ln\alpha)]^2} = O\left(\frac{df/d\rho}{\ln(\alpha/\ln\alpha)}, \quad \frac{f}{[\ln(\alpha/\ln\alpha)]^3}\right). \tag{30}$$

The expansion

$$f_{\text{inter}} = G_0 + \frac{G_1}{[\ln(\alpha/\ln\alpha)]^2} + \ldots$$

produces a first-order solution

$$G_0 = a_1 + a_2\,\mathrm{Ei}(e^{-\rho}), \tag{31}$$

for which $\lim_{\rho \to -\infty} G_0 = \lim_{R \to \kappa L_0} f_{\text{inner}}$ determines $a_1 = c_0$ and $a_2 = 0$. From the second-order equation

$$G_1 = a_3 + a_4\,\mathrm{Ei}\,(e^{-\rho}) + 6c_0\left\{\mathrm{Ei}\,(e^{-\rho})\ \mathrm{Ei}\,(-e^{-\rho}) + \int_{-\infty}^{\rho} \exp(-e^{-u})\,\mathrm{Ei}\,(e^{-u})\,du\right\}, \tag{32}$$

with $a_3 = a_4 = 0$ following from matching with f_{inner}.

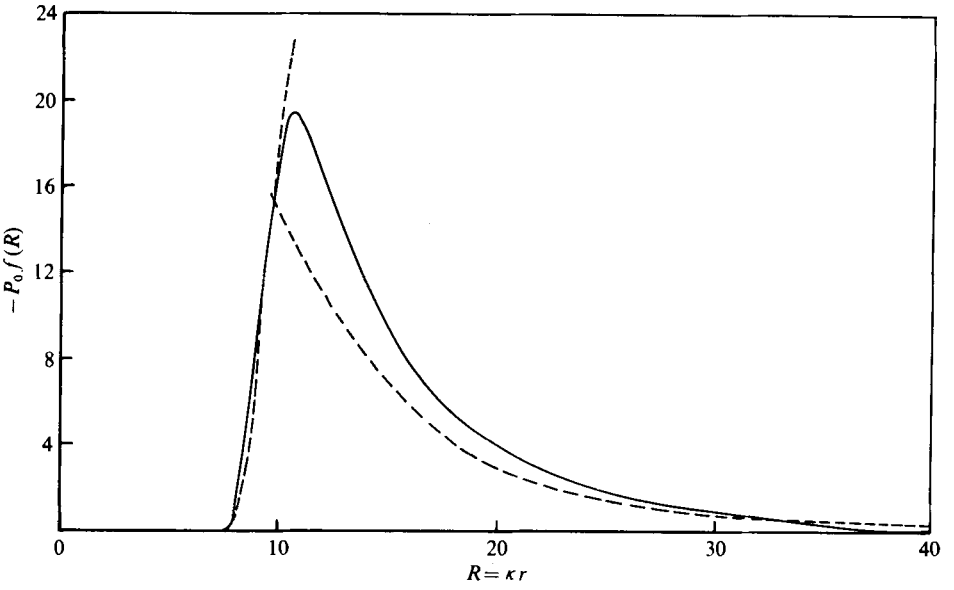

FIGURE 3. Comparison of numerical and asymptotic solutions for perturbed distribution for $\alpha = 10^5$ and $\kappa L = 9{\cdot}31$. ——, numerical solution; – – –, first-order asymptotic solution.

In the outer region the electrostatic term can be neglected to first order, so that

$$f_{\text{outer}} = b_1 R^2 + b_2/R^3. \tag{33}$$

The constants follow from the outer boundary condition (25) and the matching condition,

$$\lim_{R\to\kappa L_0} f_{\text{outer}} = \lim_{\rho\to\infty} f_{\text{inter}},$$

as

$$b_1 = -\tfrac{1}{2}, \quad b_2 = -\tfrac{1}{3}(\kappa L_0)^5, \quad c_0 = -\tfrac{5}{6}(\kappa L_0)^2. \tag{34}$$

Finally, the complete homogeneous solution is as follows.

(*a*) In the inner region $R \ll \kappa L_0$

$$f = -\tfrac{5}{6}(\kappa L_0)^2\left(1 + \alpha^{-1}\left(\frac{6}{e}\operatorname{Ei}(1+R) + c_1\right) + O(\alpha^{-2})\right). \tag{35}$$

(*b*) In the intermediate region $R = \kappa L_0 + \rho$

$$f = -\tfrac{5}{6}(\kappa L_0)^2\left\{1 + \frac{6}{(\kappa L_0)^2}\left(\operatorname{Ei}(e^{-\rho})\operatorname{Ei}(-e^{-\rho}) + \int_{-\infty}^{\rho} \exp(-e^{-u})\operatorname{Ei}(e^{-u})\,du\right) + O(\kappa L_0)^{-3}\right\}. \tag{36}$$

(*c*) In the outer region $R \gg \kappa L_0$

$$f = -\tfrac{1}{2}R^2 - \tfrac{1}{3}(\kappa L_0)^5/R^3. \tag{37}$$

This analytic approximation is compared with the previous numerical calculations for $\alpha = 10^5$ in figure 3.

The electrostatic contribution $\boldsymbol{\Sigma}^{\text{el}}$ to the particle stress can now be calculated by substituting (23) and (14) into (16) and integrating over a spherical surface to obtain

$$\boldsymbol{\Sigma}^{\text{el}} = -\frac{9}{20}\phi^2\frac{\alpha\mu_0\gamma}{(a\kappa)^5}\mathbf{E}\int_{2a\kappa}^{\infty} R(1+R)\,e^{-R}f(R)\exp\left(-\alpha\frac{e^{-R}}{R}\right)dR. \tag{38}$$

Run	$\frac{e\psi_0}{kT}$	$a\kappa$	α	$\ln\frac{\alpha}{\ln\alpha}$	ϕ^2-coefficient: Experimental: Reported (1968)	ϕ^2-coefficient: Experimental: Inter-polated (1976)	ϕ^2-coefficient: Theoretical
1	2·41	1·13	3160	5·97	319	450	376
2	2·38	1·61	11500	7·11	172	190	150
3	4·20	0·91	3990	6·18	595	—	1300
4	3·54	0·73	1760	5·46	1148	2110	2200
5	3·50	0·81	1800	5·48	466	1010	1330
6	3·34	0·81	1640	5·40	388	—	1240
7	3·50	1·45	14400	7·32	197	320	282
8	—	2·94	—	—	—	—	—
9	3·40	9·28	$4{\cdot}64\times10^{11}$	23·6	0	—	10
10	3·36	3·84	$1{\cdot}11\times10^{7}$	13·4	—	—	45
11	3·86	0·91	3370	6·03	1400	—	1160

TABLE 2. Comparison of theory with experimental data of Stone-Masui & Watillon (1968).

The two exponentials in the integrand render the contributions from the inner and outer regions negligible, leaving a single term from the intermediate region:

$$\frac{1}{\alpha}\ln\left(\frac{\alpha}{\ln(\alpha/\ln\alpha)}\right)^2\ln\frac{\alpha}{\ln\alpha}\int_{-\infty}^{\infty}(G_0(\rho)+\tfrac{1}{2}(\kappa L_0)^2)\,e^{-\rho}\exp(-e^{-\rho})\,d\rho$$
$$=-\frac{1}{3}\frac{1}{\alpha}\left(\ln\frac{\alpha}{\ln(\alpha/\ln\alpha)}\right)^4\ln\frac{\alpha}{\ln\alpha}. \quad (39)$$

Thus in the low-shear limit the suspension is isotropic and Newtonian with viscosity

$$\frac{\mu}{\mu_0}=1+\tfrac{5}{2}\beta_0\phi+\tfrac{5}{2}(\beta_0\phi)^2+\tfrac{3}{40}\ln\frac{\alpha}{\ln\alpha}\left(\ln\frac{\alpha}{\ln(\alpha/\ln\alpha)}\right)^4\frac{\phi^2}{(a\kappa)^5}\{1+O(\kappa L_0)^{-1}\}. \quad (40)$$

The last term in the viscosity agrees closely with the previous numerical solution and applies to a wider range of α. The direct Brownian contribution to the particle stress is zero in the absence of hydrodynamic interactions (Batchelor 1977).

For $a\kappa \gg 1$, (15) should be used for the electrostatic force law instead of (14). Fortunately, when $R \gg 1$ the two expressions have the same R dependence so (40) remains valid but with α given by (19). In this range the numerical solution is not valid because $a\kappa = O(1)$ was assumed to simplify the inner boundary condition. In both cases the results are valid for $\Gamma \ll (\kappa L_0)^{-1}$ provided that $L_0/a \gg 1$ to avoid hydrodynamic interactions and $L_0/a \ll 2\phi^{-\frac{1}{3}}$ to prevent multiparticle electrostatic interactions.

Stone-Masui & Watillon (1968) measured both the primary and the secondary electroviscous effects for dilute suspensions of charged polymer latex spheres with $0{\cdot}73 \leqslant a\kappa \leqslant 9{\cdot}28$, $2{\cdot}5 \leqslant e\psi_0/kT \leqslant 4{\cdot}3$ and $a \sim 3\times10^{-6}$ cm. The shear rates,

$$2\times10^{-4} \leqslant \Gamma \leqslant 2\times10^{-2},$$

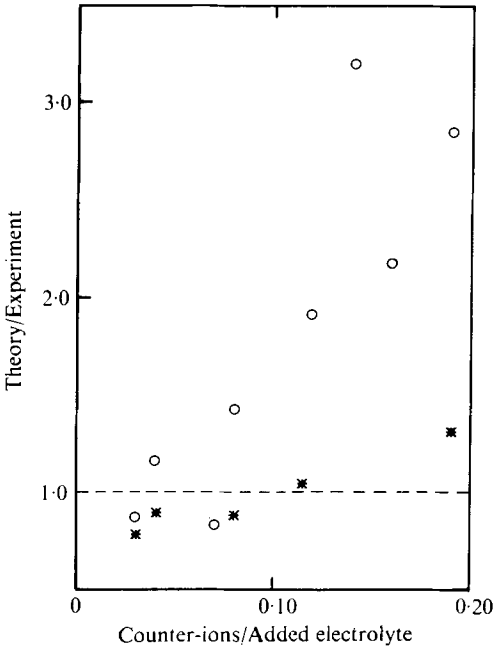

FIGURE 4. Comparison of theoretical predictions with experimental data. ○, constant added electrolyte (Stone-Masui & Watillon 1968); ✱, constant total ionic strength (Stone-Masui 1976, private communication).

and volume fractions were sufficiently low to satisfy the theoretical assumptions. Comparison of the ϕ^2-coefficient predicted by (40) with the original experimental data in table 2 reveals significant disagreement. Since the discrepancies correlate with the maximum experimental volume fraction, multiparticle electrostatic interactions were previously thought to be responsible (Russel 1976). Recently, another explanation has been proposed (Stone-Masui 1976, private communication). The reported double-layer thicknesses reflected the added electrolyte only while the counter-ions from the surface charges actually comprised a significant fraction of the total ionic strength for some runs. Since the Debye length is inversely proportional to the square root of the ionic strength while the ϕ^2-coefficient depends on $(a\kappa)^5$, the results are quite sensitive to the total electrolyte concentration. To account for the variation of counter-ion concentration with volume fraction, Stone-Masui (1976, private communication) interpolated among several runs with similar charge densities and particle sizes to obtain $\mu/\mu_0 - 1$ *vs.* ϕ at constant total ionic strength. The modified ϕ^2-coefficients which she calculated are listed in table 2. Figure 4 illustrates the effect of the counter-ions and the improved agreement.

5. Strong flows with thick double layers

As illustrated by the scaling arguments, Brownian motion can be ignored for sufficiently large shear rates. The pair conservation equation then reduces to first order and can be solved by the method of characteristics. Rather than pursue a tedious

numerical integration along three-dimensional characteristic curves, I present here analytic results for one limiting case.

For thick double layers ($a\kappa \ll 1$) the linear-superposition approximation is appropriate and for

$$\Gamma \gg \left(\ln \frac{\alpha}{\ln(\alpha/\ln \alpha)}\right)^{-1}$$

equation (20) simplifies to

$$\left\{\alpha \frac{1+R}{R^3} e^{-R}\mathbf{R} + \Gamma(\boldsymbol{\Omega}+\mathbf{E}).\mathbf{R}\right\}.\nabla_R P = \alpha \frac{e^{-R}}{R} P. \tag{41}$$

In spherical co-ordinates the characteristic curves are defined by

$$\left.\begin{aligned} \frac{dR}{ds} &= \alpha \frac{1+R}{R^2} e^{-R} + \Gamma \frac{\mathbf{R}.\mathbf{E}.\mathbf{R}}{R}, \\ \frac{d\theta}{ds} = \frac{u_\theta}{R}, \quad \frac{d\phi}{ds} &= \frac{u_\phi}{R\sin\theta}, \quad \frac{dP}{ds} = \alpha \frac{e^{R}}{R} P, \end{aligned}\right\} \tag{42}$$

where u_θ and u_ϕ represent the dimensionless angular components of the imposed flow

$$\mathbf{u} = (\mathbf{E}+\boldsymbol{\Omega}).\mathbf{R}. \tag{43}$$

The first three equations determine the trajectories of the interacting pair and the last the variation of P along these trajectories. s will be chosen to measure arc length downstream from the point at which $u_r = 0$. As $s \to -\infty$

$$R \to \infty, \quad \phi, \theta \to \text{constants}, \quad P \to n,$$

which corresponds to a uniform distribution upstream.

Again hydrodynamic interactions are ignored, leaving only the electrostatic force to displace the spheres from the fluid streamlines. Since $d\theta/ds$ and $d\phi/ds$ are unaffected, $\theta(s)$ and $\phi(s)$ can be obtained independently from R and substituted into (42) to provide

$$\frac{dR}{ds} = \alpha \frac{1+R}{R^2} e^{-R} + \Gamma R G(s), \tag{44}$$

where $G(s)$ follows from $\theta(s)$ and $\phi(s)$.

The minimum separation κL mentioned above is determined by

$$dR/ds = 0,$$

or

$$\frac{(\kappa L)^3}{1+\kappa L} e^{\kappa L} \sim \frac{\alpha}{\Gamma}. \tag{45}$$

Below we analyse the case

$$\kappa L \sim (\alpha/\Gamma)^{\frac{1}{3}} \ll 1, \tag{46}$$

for which the exponential in (44) can be linearized, so that

$$\frac{dR}{ds} = \frac{\alpha}{R^2} + \Gamma R G(s) \tag{47}$$

with $$R^3 = \exp\left(3\Gamma\int_0^s G(t)\,dt\right)\left\{R_0^3 + 3\alpha\int_0^s \exp\left(-3\Gamma\int_0^u G(t)\,dt\right)du\right\}, \tag{48}$$

where R_0 is an integration constant. Unfortunately, $G(s)$ cannot be evaluated for a general linear flow, so simple shear and uniform straining have been chosen to illustrate the rheology.

(*a*) *Simple shear*

$$\left.\begin{aligned} \nabla\mathbf{u} &= 2^{\frac{1}{2}}\gamma\begin{pmatrix}0&1&0\\0&0&0\\0&0&0\end{pmatrix},\\ u_r &= 2^{\frac{1}{2}}R\sin^2\theta\sin\phi\cos\phi,\\ u_\theta = 2^{\frac{1}{2}}R\sin\theta\cos\theta\sin\phi\cos\phi,&\quad u_\phi = -2^{\frac{1}{2}}R\sin\theta\sin^2\phi, \end{aligned}\right\} \tag{49}$$

$$\left.\begin{aligned} \cos\theta &\to \frac{Z}{[Z^2+Y^2(1+(\Gamma s)^2)]^{\frac{1}{2}}}\\ \sin\phi &\to \frac{1}{(1+(\Gamma s)^2)^{\frac{1}{2}}}\\ R &\to [Z^2+Y^2(1+(\Gamma s)^2)]^{\frac{1}{2}} = R_\infty \end{aligned}\right\} \quad \text{as} \quad s\to-\infty,$$

$$G(s) = \frac{2^{\frac{1}{2}}sY^2}{Z^2+Y^2(1+(\Gamma s)^2)}, \tag{50}$$

with solution

$$R^3 = R_\infty^3\left\{1+\frac{3\alpha}{2^{\frac{1}{2}}\Gamma Y(Y^2+Z^2)}\left(1+\frac{Y\Gamma s}{R_\infty}\right)\right\}. \tag{51}$$

(*b*) *Uniform straining*

$$\left.\begin{aligned} \nabla\mathbf{u} &= \frac{2}{6^{\frac{1}{2}}}\gamma\begin{pmatrix}-\frac{1}{2}&0&0\\0&-\frac{1}{2}&0\\0&0&1\end{pmatrix},\\ u_r &= \tfrac{1}{2}\times 6^{\frac{1}{2}}R(\cos^2\theta-\tfrac{1}{2}\sin^2\theta),\\ u_\theta = -\tfrac{1}{2}\times 6^{\frac{1}{2}}R\sin\theta\cos\theta,&\quad u_\phi = 0, \end{aligned}\right\} \tag{52}$$

$$\left.\begin{aligned} \cos\theta &\to [1+\exp(-6^{\frac{1}{2}}\Gamma s)]^{-\frac{1}{2}}\\ R &\to \exp(\tfrac{1}{3}\times 6^{\frac{1}{2}}\Gamma s)\,[1+\exp(-6^{\frac{1}{2}}\Gamma s)]^{\frac{1}{2}} \end{aligned}\right\} \quad \text{as} \quad s\to-\infty.$$

$$G(s) = \frac{6^{\frac{1}{2}}}{3}\,\frac{1-\frac{1}{2}\exp(-6^{\frac{1}{2}}\Gamma s)}{1+\exp(-6^{\frac{1}{2}}\Gamma s)}, \tag{53}$$

with solution

$$R^3 = \frac{3^{\frac{1}{2}}\alpha}{\Gamma}\rho^3\exp(6^{\frac{1}{2}}\Gamma s)\,[1+\exp(-6^{\frac{1}{2}}\Gamma s)]^{\frac{3}{2}}\left\{1-\frac{1}{\rho^3}\left(1-\frac{2^{\frac{1}{2}}}{[1+\exp(-6^{\frac{1}{2}}\Gamma s)]^{\frac{1}{2}}}\right)\right\}. \tag{54}$$

The constants of integration define the upstream location of the trajectory (Y, Z) for simple shear and the radius ρ at $s = 0$ or $\theta = \frac{1}{4}\pi$,

$$R = 2\times 6^{\frac{1}{2}}\alpha\Gamma^{-1}\rho,$$

for uniform straining. For the latter a single constant suffices because of the axial symmetry.

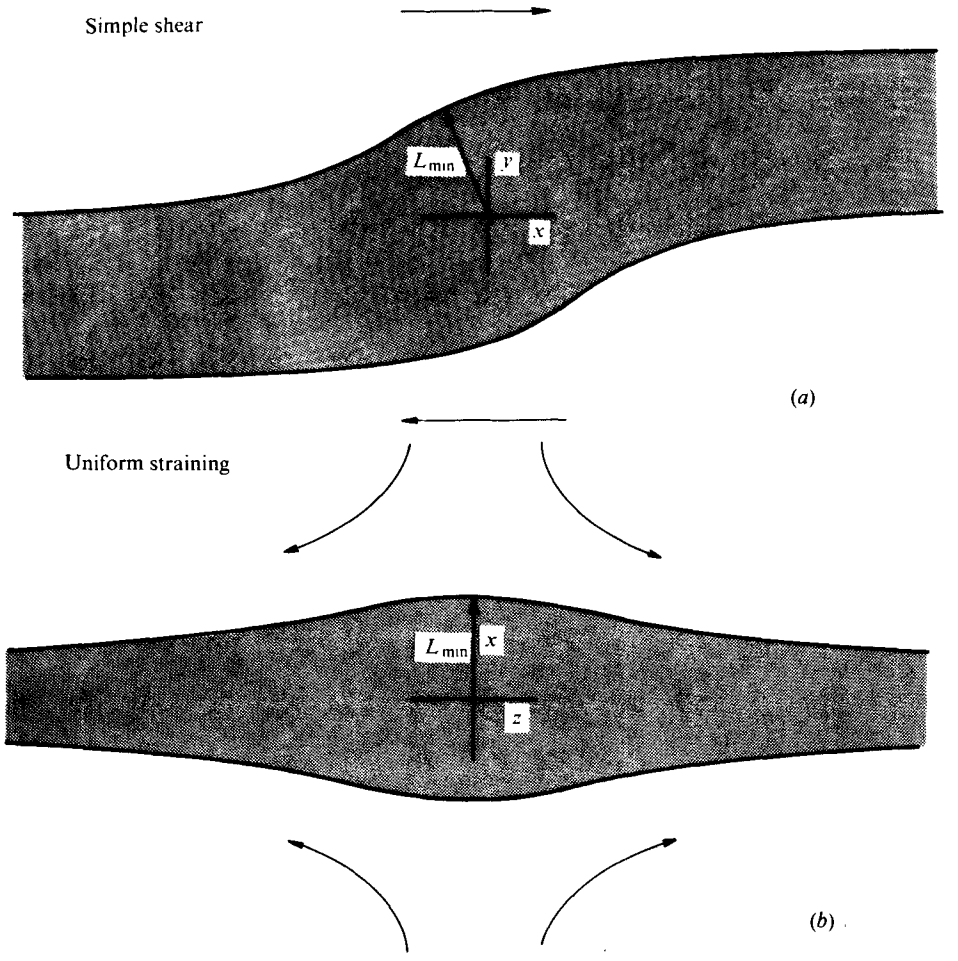

FIGURE 5. Limiting streamlines for strong flows $\alpha \ll \Gamma \ll \alpha/(a\kappa)^3$ for $a\kappa \ll 1$. (*a*) Simple shear. (*b*) Uniform straining.

Two interesting aspects of the trajectories are the minimum separation and the shadow zone depleted of particles by the electrostatic force. Approach along the line of centres defines

$$\kappa L_{\min} = 1{\cdot}18(\alpha/\Gamma)^{\frac{1}{3}} \tag{55}$$

at $Y = Z = 0$ for simple shear,

$$\kappa L_{\min} = 1{\cdot}35(\alpha/\Gamma)^{\frac{1}{3}} \tag{56}$$

at $\theta = \frac{1}{2}\pi$ for uniform straining and

$$\kappa L_{\min} = 1{\cdot}07(\alpha/\Gamma)^{\frac{1}{3}} \tag{57}$$

at $\theta = 0, \pi$ for axisymmetric compression (pure straining with the signs reversed). The limiting streamlines in figure 5 illustrate the shadow zones although far downstream Brownian motion would eventually eliminate the concentration difference.

From (42) the variation in P along a trajectory is

$$\ln \frac{P}{n} = \alpha \int_{-\infty}^{s} \frac{e^{-R}}{R} dt. \tag{58}$$

The dominant effect comes from

$$R \sim (\alpha/\Gamma)^{\frac{1}{3}} \ll 1,$$

near the minimum separation; but $dt \sim 1/\Gamma$, so that

$$P \sim n[1 + O(\alpha/\Gamma)^{\frac{2}{3}}]. \tag{59}$$

A similar conclusion follows from a complete analysis including the singularities due to vanishingly small velocities at $Y = 0$ (simple shear) and $\theta = \frac{1}{2}\pi$ (straining), and allows P to be considered constant for first-order calculations of the bulk stress.

From (16) the deviatoric portion of the electrical particle stress is

$$\mathbf{\Sigma}^{\mathrm{el}} = -\frac{3\phi}{8\pi a^3}\int(\mathbf{nn} - \tfrac{1}{3}\boldsymbol{\delta})\, r F_{\mathrm{el}}(r)\, P(\mathbf{r})\, d^3\mathbf{r}, \tag{60}$$

where $\mathbf{n} = \mathbf{r}/r$. The shadow zone, in which $P = 0$, can be removed from the integral and the remaining volume mapped onto a curvilinear co-ordinate system conforming to the trajectories. Then integration can proceed along each trajectory emanating from upstream infinity using the volume elements derived in appendix A.

For simple shear with

$$\mathscr{Y} = Y\left(\frac{2^{\frac{1}{2}}\Gamma}{3\alpha}\right)^{\frac{1}{3}}, \quad \mathscr{Z} = Z\left(\frac{2^{\frac{1}{2}}\Gamma}{3\alpha}\right)^{\frac{1}{3}}, \quad \mathscr{X} = Y\Gamma s, \quad \mathscr{R} = R\left(\frac{2^{\frac{1}{2}}\Gamma}{3\alpha}\right)^{\frac{1}{3}}, \tag{61}$$

F_{el} given by (14), and the volume element (A 9),

$$\mathbf{\Sigma}^{\mathrm{el}} = -0{\cdot}443\,\mu_0\gamma\frac{\phi^2}{(a\kappa)^5}\left(\frac{\alpha}{\Gamma}\right)^{\frac{5}{3}}\int(\mathbf{nn} - \tfrac{1}{3}\boldsymbol{\delta})\frac{1 + (3\alpha/2^{\frac{1}{2}}\Gamma)^{\frac{1}{3}}\mathscr{R}}{\mathscr{R}}\exp[-(3\alpha/2^{\frac{1}{2}}\Gamma)^{\frac{1}{3}}\mathscr{R}]\,d\mathscr{X}\,d\mathscr{Y}\,d\mathscr{Z}. \tag{62}$$

Without the electrostatic force the particles would follow

$$\mathscr{R} = \mathscr{R}_\infty = (\mathscr{X}^2 + \mathscr{Y}^2 + \mathscr{Z}^2)^{\frac{1}{2}} \tag{63}$$

and (62) would reduce to zero since

$$\int \mathbf{nn}\, d\mathscr{X}\, d\mathscr{Y} d\mathscr{Z} = \tfrac{1}{3}\boldsymbol{\delta}\int d\mathscr{X}\, d\mathscr{Y}\, d\mathscr{Z}. \tag{64}$$

Thus the non-zero deviatoric particle stresses are directly related to the asymmetry in the trajectories; to hasten the numerical convergence of the integrals the unperturbed path has been subtracted from the integrand.

The major contribution arises from the inner region in which

$$(\alpha/\Gamma)^{\frac{1}{3}}\mathscr{R} \ll 1.$$

The integral over this region converges, allowing the outer region to be ignored to first order, for all stresses except $\Sigma_{11}^{\mathrm{el}}$. In this case the exponential deaay of the force in the outer region must be included downstream, where $\mathscr{R} \gg 1$ and

$$\mathscr{R} \sim \mathscr{X}[1 + 2/\mathscr{Y}(\mathscr{Y}^2 + \mathscr{Z}^2)]^{\frac{1}{3}}. \tag{65}$$

The final results for the shear stress and the two normal-stress differences are (see appendix B for details)

$$\Sigma_{12}^{\mathrm{el}} = 1{\cdot}30\,\phi^2 \frac{\mu_0\gamma}{(a\kappa)^5}\left(\frac{\alpha}{\Gamma}\right)^{\frac{5}{3}}, \tag{66a}$$

$$N_1 = \Sigma_{11}^{\mathrm{el}} - \Sigma_{22}^{\mathrm{el}} = 1{\cdot}61\phi^2 \frac{\epsilon\psi_0^2\kappa^2}{(a\kappa)^4}\left(\frac{\alpha}{\Gamma}\right)^{\frac{2}{3}} \ln\frac{\alpha}{\Gamma}\left(1 - \frac{1{\cdot}83}{\ln\dfrac{\alpha}{\Gamma}}\right), \tag{66b}$$

$$N_2 = \Sigma_{22}^{\mathrm{el}} - \Sigma_{33}^{\mathrm{el}} = -2{\cdot}61\phi^2 \frac{\epsilon\psi_0^2\kappa^2}{(a\kappa)^4}\left(\frac{\alpha}{\Gamma}\right)^{\frac{2}{3}}. \tag{66c}$$

The complete shear viscosity is

$$\frac{\mu_{\mathrm{sh}}}{\mu_0} = 1 + \tfrac{5}{2}\beta_0\phi + \tfrac{5}{2}(\beta_0\phi)^2 + 0{\cdot}92\frac{\phi^2}{(a\kappa)^5}\left(\frac{\alpha}{\Gamma}\right)^{\frac{5}{3}}, \tag{67}$$

which is remarkably close to the value $\Sigma/\mu_0\gamma$ from the scale analysis.

For uniform straining the scaled co-ordinates are

$$\tau = 6^{\frac{1}{2}}\Gamma s, \quad \mathscr{R} = (\Gamma/3^{\frac{1}{2}}\alpha)^{\frac{1}{3}}R, \tag{68}$$

so that

$$\boldsymbol{\Sigma}^{\mathrm{el}} = -0{\cdot}386\mu_0\gamma\left(\frac{\alpha}{\Gamma}\right)^{\frac{5}{3}}\frac{\phi^2}{(a\kappa)^5}\int_1^\infty\int_{-\infty}^{\infty}\int_0^{2\pi}(\mathbf{nn} - \tfrac{1}{3}\boldsymbol{\delta}) \times \frac{1 + (3^{\frac{1}{2}}\alpha/\Gamma)^{\frac{1}{3}}\mathscr{R}}{\mathscr{R}}\exp[-(3^{\frac{1}{2}}\alpha/\Gamma)^{\frac{1}{3}}\mathscr{R}]\,\rho^2\,d\phi\,d\tau\,d\rho. \tag{69}$$

Because of the symmetry

$$\Sigma_{11}^{\mathrm{el}} = \Sigma_{22}^{\mathrm{el}} = -\tfrac{1}{2}\Sigma_{33}^{\mathrm{el}} \tag{70}$$

and as shown in appendix B

$$\Sigma_{33}^{\mathrm{el}} = 1{\cdot}43\mu_0\gamma\frac{\phi^2}{(a\kappa)^5}\left(\frac{\alpha}{\Gamma}\right)^{\frac{5}{3}}. \tag{71}$$

The effective extensional viscosity

$$\frac{\mu_{\mathrm{ext}}}{\mu_0} = \frac{\Sigma_{33} - \frac{1}{2}(\Sigma_{11} + \Sigma_{22})}{\mu_0\gamma E_{33}} = 3{\cdot}0 + \tfrac{1{\cdot}5}{2}\beta_0\phi + \tfrac{1{\cdot}5}{2}(\beta_0\phi)^2 + 2{\cdot}64\left(\frac{\alpha}{\Gamma}\right)^{\frac{5}{3}}\frac{\phi^2}{(a\kappa)^5} \tag{72}$$

indicates that $\mu_{\mathrm{ext}} \approx 3\mu_{\mathrm{sh}}$ as for Newtonian fluids while the strain-rate dependence is definitely non-Newtonian.

As indicated earlier these results pertain to a rather restricted range of strain rates. The strong electrostatic interactions occur only for $\Gamma > \alpha$ while $\Gamma < \alpha/(a\kappa)^3$ is necessary for hydrodynamic interactions to be negligible. Such conditions could be obtained at low ionic strengths ($\kappa^{-1} \sim 0{\cdot}1\,\mu$m) with small ($\sim 0{\cdot}02\,\mu$m) particles having moderate surface potentials ($e\psi_0/kT \sim 1$–2) subjected to high shear rates ($\sim 10^4\,\mathrm{s}^{-1}$). The qualitative trends, however, should reflect the non-Newtonian nature of the suspension over a wider range.

6. Discussion

Since only two limiting cases have been analysed, this work can offer no constitutive equation to describe the rheology of colloidal suspensions. Nonetheless, several interesting features of electrostatically dilute suspensions of charged particles are suggested:

(*a*) An isotropic, Newtonian zero-shear limit which is quite sensitive to the ionic strength.

(*b*) Strain-thinning and non-zero normal stresses characterized by at least two relaxation times.

(*c*) A Newtonian state at high shear.

This represents a qualitative difference from the rheology predicted for polymer solutions by various molecular models: random coils (Lodge & Wu 1971), elastic particles (Hinch 1971), slender rods (Hinch & Leal 1972) and dumbbells (Bird *et al.* 1971). In particular, the extensional viscosity decreases with increasing rate of strain and apparently Trouton's ratio remains ≈ 3. On the other hand, with $N_1 \neq 0$ these fluids are not purely viscous but do exhibit memory, or elastic effects. While no surprise, these results deserve emphasis because of the prevailing orientation of rheology towards polymers.

In the strong-flow limit hydrodynamic interactions would appear to dominate the colloidal forces. In flows with closed streamlines such as simple shear, however, the latter can still affect the permanent doublets (Batchelor & Green 1972). Indeed strong electrostatic repulsions should eliminate doublets entirely with an $O(1)$ effect on the ϕ^2-coefficient of the viscosity (Hinch 1976).

These results remain rigorously valid only for dilute or moderately dilute systems, but are sufficiently large to be measurable as well as providing qualitative information about higher concentrations.

This work was initiated during a NATO Postdoctoral Fellowship with Prof. G. K. Batchelor at Cambridge University. The author is indebted also to Dr E. J. Hinch for his stimulating ideas and mathematical assistance at key points. Completion of the work was supported by the National Science Foundation through Grant no. ENG 75-10557.

Appendix A. Volume elements

Calculation of volume elements for the non-orthogonal curvilinear co-ordinate systems (q_1, q_2, q_3) is straightforward but tedious. From Happel & Brenner (1965, appendix A), the basis vectors

$$\mathbf{e}_i = \partial \mathbf{R}/\partial q_i \tag{A 1}$$

and the metric coefficients

$$g_{ij} = \mathbf{e}_i \cdot \mathbf{e}_j \tag{A 2}$$

are needed to obtain the volume element

$$dV = dx\,dy\,dz = |g_{ij}|^{\frac{1}{2}} dq_1\,dq_2\,dq_3, \tag{A 3}$$

where $|\ |$ denotes the determinant.

For simple shear first let $(q_1, q_2, q_3) = (\tau, \mathscr{Y}, \nu)$, where

$$\tau = \Gamma s, \quad \mathscr{Y} = Y(2^{\frac{1}{2}}\Gamma/3\alpha)^{\frac{1}{2}}, \quad \nu = Z/Y. \tag{A 4}$$

Then $\mathscr{R} = x\mathbf{i} + y\mathbf{j} + z\mathbf{k}$ with

$$\left.\begin{aligned} \frac{x}{\mathscr{R}} &= \frac{\tau}{(1+\nu^2+\tau^2)^{\frac{1}{2}}}, \quad \frac{y}{\mathscr{R}} = \frac{1}{(1+\nu^2+\tau^2)^{\frac{1}{2}}}, \quad \frac{z}{\mathscr{R}} = \frac{\nu}{(1+\nu^2+\tau^2)^{\frac{1}{2}}}, \\ \mathscr{R}^3 &= (1+\nu^2+\tau^2)^{\frac{3}{2}} \left\{ \mathscr{Y}^3 + \frac{1}{1+\nu^2}\left(1 + \frac{\tau}{(1+\nu^2+\tau^2)^{\frac{1}{2}}}\right)\right\}. \end{aligned}\right\} \tag{A 5}$$

From the basis vectors

$$\mathbf{e}_{\mathscr{Y}} = \frac{\partial\mathscr{R}/\partial\mathscr{Y}}{(1+\nu^2+\tau^2)^{\frac{1}{2}}}(\tau\mathbf{i}+\mathbf{j}+\nu\mathbf{k}), \tag{A 6a}$$

$$\begin{aligned}\mathbf{e}_{\nu} = {} & \mathbf{i}\left(\frac{\partial\mathscr{R}}{\partial\nu}\frac{\tau}{(1+\nu^2+\tau^2)^{\frac{1}{2}}} - \frac{\nu\tau\mathscr{R}}{(1+\nu^2+\tau^2)^{\frac{3}{2}}}\right) \\ & + \mathbf{j}\left(\frac{\partial\mathscr{R}}{\partial\nu}\frac{1}{(1+\nu^2+\tau^2)^{\frac{1}{2}}} - \frac{\nu\mathscr{R}}{(1+\nu^2+\tau^2)^{\frac{3}{2}}}\right) \\ & + \mathbf{k}\left(\frac{\partial\mathscr{R}}{\partial\nu}\frac{\nu}{(1+\nu^2+\tau^2)^{\frac{1}{2}}} - \frac{(1+\tau^2)\mathscr{R}}{(1+\nu^2+\tau^2)^{\frac{3}{2}}}\right),\end{aligned} \tag{A 6b}$$

$$\mathbf{e}_{\tau} = \frac{1}{\mathscr{R}^2(1+\nu^2+\tau^2)^{\frac{1}{2}}}((\mathscr{R}^3+\tfrac{1}{3}\tau)\,\mathbf{i}+\tfrac{1}{3}\mathbf{j}+\tfrac{1}{3}\nu\mathbf{k})), \tag{A 6c}$$

the metric coefficients and

$$|g_{ij}| = \left(\frac{\partial\mathscr{R}}{\partial\mathscr{Y}}\right)^2\frac{\mathscr{R}^4}{(1+\nu^2+\tau^2)^3} \tag{A 7}$$

can be calculated. With

$$3\mathscr{R}^2\,\partial\mathscr{R}/\partial\mathscr{Y} = 3\mathscr{Y}^2(1+\nu^2+\tau^2)^{\frac{3}{2}} \tag{A 8}$$

the volume element becomes

$$\mathscr{R}^2\sin\theta\,d\mathscr{R}\,d\theta\,d\phi = \mathscr{Y}^2 d\tau\,d\mathscr{Y}\,d\nu = d\mathscr{X}\,d\mathscr{Y}\,d\mathscr{Z}, \tag{A 9}$$

where $\mathscr{X} = \mathscr{Y}\tau$.

For uniform straining the appropriate co-ordinates are (τ, ρ, ϕ), where

$$\tau = 6^{\frac{1}{2}}\Gamma s,$$

$$\mathscr{R} = \left(\frac{\Gamma}{3^{\frac{1}{2}}\alpha}\right)^{\frac{1}{3}}\mathscr{R},$$

$$\mathscr{R} = x\mathbf{i}+y\mathbf{j}+z\mathbf{k}$$

and

$$\frac{x}{\mathscr{R}} = \frac{\exp(-\frac{1}{2}\tau)}{[1+\exp(-\tau)]^{\frac{1}{2}}}\sin\phi, \tag{A 10a}$$

$$\frac{y}{\mathscr{R}} = \frac{\exp(-\frac{1}{2}\tau)}{[1+\exp(-\tau)]^{\frac{1}{2}}}\cos\phi, \tag{A 10b}$$

$$\frac{z}{\mathscr{R}} = \frac{1}{[1+\exp(-\tau)]^{\frac{1}{2}}}, \tag{A 10c}$$

$$\mathscr{R}^3 = \rho^3\exp(\tau)\,[1+\exp(-\tau)]^{\frac{3}{2}}\left[1-\frac{1}{\rho^3}\left(1-\frac{2^{\frac{1}{2}}}{[1+\exp(-\tau)]^{\frac{1}{2}}}\right)\right]. \tag{A 10d}$$

Again from the basis vectors

$$\left.\begin{aligned}\mathbf{e}_{\tau} &= -\left\{\left(1-\frac{2^{\frac{1}{2}}}{\mathscr{R}^3}\right)x\mathbf{i}+\left(1-\frac{2^{\frac{1}{2}}}{\mathscr{R}^3}\right)y\mathbf{j}-\left(2+\frac{2^{\frac{1}{2}}}{\mathscr{R}^3}\right)z\mathbf{k}\right\}, \\ \mathbf{e}_{\rho} &= \frac{\partial\mathscr{R}}{\partial\rho}\left(\frac{x}{\mathscr{R}}\mathbf{i}+\frac{y}{\mathscr{R}}\mathbf{j}+\frac{z}{\mathscr{R}}\mathbf{k}\right), \quad \mathbf{e}_{\phi} = -y\mathbf{i}+x\mathbf{j}\end{aligned}\right\} \tag{A 11}$$

and the metric coefficients, one can calculate

$$|g_{ji}| = \mathscr{R}^4\left(\frac{\partial\mathscr{R}}{\partial\rho}\right)^2\frac{\exp(-2\tau)}{[1+\exp(-\tau)]^3}. \tag{A 12}$$

Since

$$\mathscr{R}^2\frac{\partial\mathscr{R}}{\partial\rho} = \rho^2\exp(\tau)\,[1+\exp(-\tau)]^{\frac{3}{2}} \tag{A 13}$$

one has $$|g_{ij}| = \rho^4 \tag{A 14}$$

and $$dV = \mathscr{R}^2 \sin\theta \, d\mathscr{R} \, d\theta \, d\phi = \rho^2 \, d\tau \, d\rho \, d\phi. \tag{A 15}$$

Appendix B. Evaluation of particle stresses

The first normal-stress difference N_1 for simple shear and Σ_{33}^{el} for uniform straining require careful calculation because the integrals (62) and (69) over the inner region alone diverge. Thus the exponentially decaying force must be retained in the outer region to remove the divergence.

For simple shear

$$N_1 = -0{\cdot}443\,\mu_0\gamma\frac{\phi^2}{(a\kappa)^5}\left(\frac{\alpha}{\Gamma}\right)^{\frac{5}{3}}(I_1+I_2), \tag{B 1}$$

where

$$\left.\begin{aligned} I_1 &= \int_{-\infty}^{\bar{\mathscr{X}}}\int_A \frac{\mathscr{X}^2-\mathscr{Y}^2}{\mathscr{R}^2}\left(\frac{1}{\mathscr{R}}-\frac{1}{\mathscr{R}_\infty}\right)dA\,d\mathscr{X}, \\ I_2 &= \int_{\bar{\mathscr{X}}}^{\infty}\int_A \left\{\frac{1+(3\alpha/2^{\frac{1}{2}}\Gamma)^{\frac{1}{3}}\mathscr{X}\delta}{\mathscr{X}\delta}\exp[-(3\alpha/2^{\frac{1}{2}}\Gamma)^{\frac{1}{3}}\mathscr{X}\delta]\right. \\ &\qquad \left. -\frac{1+(3\alpha/2^{\frac{1}{2}}\Gamma)^{\frac{1}{3}}\mathscr{X}}{\mathscr{X}}\exp[-(3\alpha/2^{\frac{1}{2}}\Gamma)^{\frac{1}{3}}\mathscr{X}]\,dA\,d\mathscr{X}, \right. \\ \delta &= \left(1+\frac{2}{\mathscr{Y}(\mathscr{Y}^2+\mathscr{X}^2)}\right)^{\frac{1}{2}}, \quad dA = d\mathscr{Y}\,d\mathscr{Z}, \end{aligned}\right\} \tag{B 2}$$

with $\bar{\mathscr{X}} \gg 1$. I_2 can be integrated once analytically to obtain

$$\begin{aligned} I_2 = \int_A \left\{\frac{1}{\delta}E_1\left(\left(\frac{3\alpha}{2^{\frac{1}{2}}\Gamma}\right)^{\frac{1}{3}}\bar{\mathscr{X}}\delta\right) + \frac{\exp[-(3\alpha/2^{\frac{1}{2}}\Gamma)^{\frac{1}{3}}\bar{\mathscr{X}}\delta]}{\delta_\infty}\right. \\ \left. - E_1\left(\left(\frac{3\alpha}{2^{\frac{1}{2}}\Gamma}\right)^{\frac{1}{3}}\bar{\mathscr{X}}\right) - \exp[-(3\alpha/2^{\frac{1}{2}}\Gamma)^{\frac{1}{3}}\bar{\mathscr{X}}]\right\}, \end{aligned} \tag{B 3}$$

where $$E_1(x) = \int_x^\infty \frac{e^{-t}}{t}\,dt,$$

and then expanded for $(3\alpha/2^{\frac{1}{2}}\Gamma)^{\frac{1}{3}}\bar{\mathscr{X}} \ll 1$ as

$$I_2 = \left(\ln\bar{\mathscr{X}} + \tfrac{1}{3}\ln\frac{\alpha}{\Gamma} - 0{\cdot}172\right)\int_A\left(1-\frac{1}{\delta}\right)dA - \int_A \frac{\ln\delta}{\delta}\,dA. \tag{B 4}$$

I_1 can be split into integrals over $-\infty < \mathscr{X} < \mathscr{X}_0$ and $\mathscr{X}_0 < \mathscr{X} < \bar{\mathscr{X}}$ with $\mathscr{X}_0 \gg 1$ and the second integrated analytically to obtain

$$I_1 = \int_{-\infty}^{\mathscr{X}_0}\int_A \frac{\mathscr{X}^2-\mathscr{Y}^2}{\mathscr{R}^2}\left(\frac{1}{\mathscr{R}}-\frac{1}{\mathscr{R}_\infty}\right)dA\,d\mathscr{X} + (\ln\bar{\mathscr{X}} - \ln\mathscr{X}_0)\int_A\left(\frac{1}{\delta}-1\right)dA. \tag{B 5}$$

Now when I_1 and I_2 are summed the $\ln\bar{\mathscr{X}}$ terms will cancel.

The remaining integrals have been calculated numerically as

$$\left.\begin{aligned} \int_A\left(1-\frac{1}{\delta}\right)dA &= 22{\cdot}6, \quad \int_A\frac{\ln\delta}{\delta}\,dA = 19{\cdot}4, \\ \int_\infty^{100}\int_A \frac{\mathscr{X}^2-\mathscr{Y}^2}{\mathscr{R}^2}\left(\frac{1}{\mathscr{R}}-\frac{1}{\mathscr{R}_\infty}\right)dA\,d\mathscr{X} &= -59{\cdot}7. \end{aligned}\right\} \tag{B 6}$$

Substitution of the above results into (B 1) provides the formula (66*b*) for N_1.

For uniform straining (69) can be written as

$$\Sigma_{33}^{\mathrm{el}} = -0{\cdot}808\,\mu_0\gamma\frac{\phi^2}{(a\kappa)^5}\left(\frac{\alpha}{\Gamma}\right)^{\frac{5}{3}}(I_3+I_4), \tag{B 7}$$

where

$$I_3 = \int_1^{\bar\rho}\int_{-\infty}^{\infty}\frac{2-e^{-\tau}}{1+e^{-\tau}}\frac{\rho^2}{\mathscr{R}}d\tau\,d\rho, \tag{B 8}$$

$$I_4 = \int_{\bar\rho}^{\infty}\int_{-\infty}^{\infty}\frac{2-e^{-\tau}}{1+e^{-\tau}}\frac{1+(3\tfrac{1}{2}\alpha/\Gamma)^{\frac{1}{3}}\mathscr{R}}{\mathscr{R}}\exp\left[-(3\tfrac{1}{2}\alpha/\Gamma)^{\frac{1}{3}}\mathscr{R}\right]\rho^2\,d\tau\,d\rho. \tag{B 9}$$

I_3 can be integrated over ρ and then expanded for $\bar\rho \gg 1$ to produce

$$I_3 = \tfrac{1}{2}\bar\rho^2\int_{-\infty}^{\infty}\frac{e^{-\frac{1}{3}\tau}(2-e^{-\tau})}{(1+e^{-\tau})^{\frac{3}{2}}} - 0{\cdot}630\int_{-\infty}^{\infty}\frac{e^{-\frac{1}{3}\tau}(2-e^{-\tau})}{(1+e^{-\tau})^{\frac{11}{6}}}d\tau, \tag{B 10}$$

where the second integral is numerically equal to 2·81. In the outer region the trajectories are undisturbed to first order, i.e.

$$\mathscr{R} = \rho e^{\frac{1}{3}\tau}(1+e^{-\tau})^{\frac{1}{2}}, \tag{B 11}$$

while $(3\tfrac{1}{2}\alpha/\Gamma)^{\frac{1}{3}}\bar\rho \ll 1$, so

$$I_4 = -\tfrac{1}{2}\bar\rho^2\int_{-\infty}^{\infty}\frac{e^{-\frac{1}{3}\tau}(2-e^{-\tau})}{(1+e^{-\tau})^{\frac{3}{2}}}d\tau + 2{\cdot}08\left(\frac{\Gamma}{\alpha}\right)^{\frac{2}{3}}\int_{-\infty}^{\infty}\frac{e^{-\tau}(2-e^{-\tau})}{(1+e^{-\tau})^{\frac{5}{2}}}d\tau. \tag{B 12}$$

When I_3 and I_4 are summed the $\bar\rho^2$ terms cancel while the second term of I_4 integrates to zero, leaving (71).

REFERENCES

Batchelor, G. K. 1970 *J. Fluid Mech.* **41**, 545.

Batchelor, G. K. 1975 *J. Fluid Mech.* **74**, 1.

Batchelor, G. K. 1977 *J. Fluid Mech.* **83**, 97.

Batchelor, G. K. & Green, J. T. 1972 *J. Fluid Mech.* **56**, 401.

Bell, G. M., Levine, S. & McCartney, L. N. 1970 *J. Colloid Interface Sci.* **33**, 335.

Bell, G. M. & Peterson, G. C. 1972 *J. Colloid Interface Sci.* **41**, 542.

Bird, R. B., Warner, H. R. & Evans, D. C. 1971 *Fortschritte der Hochpolymeren-Forschung* **8**, 1.

Booth, F. 1950 *Proc. Roy. Soc.* A **203**, 533.

Booth, F. 1954 *J. Chem. Phys.* **22**, 1956.

Chan, F. S., Blachford, J. & Goring, D. A. I. 1966 *J. Colloid Interface Sci.* **22**, 378.

Freundlich, H. & Jones, A. D. 1936 *J. Phys. Chem.* **40**, 1217.

Fryling, C. F. 1963 *J. Colloid Interface Sci.* **18**, 713.

Happel, J. & Brenner, H. 1965 *Low Reynolds Number Hydrodynamics.* Prentice-Hall.

Hinch, E. J. 1971 The mechanics of suspensions of particles in fluids. Ph.D. thesis, University of Cambridge.

Hinch, E. J. 1976 *Brit. Soc. Rheol. Meeting, Bristol.*

Hinch, E. J. & Leal, L. G. 1972 *J. Fluid Mech.* **52**, 683.

Hoffman, R. L. 1972 *Trans. Soc. Rheol.* **16**, 155.

Hoffman, R. L. 1974 *J. Colloid Interface Sci.* **46**, 491.

Honig, E. P., Roebersen, G. J. & Wiersema, P. H. 1971 *J. Colloid Interface Sci.* **36**, 97.

Jeffrey, D. J. & Acrivos, A. 1976 *A.I.Ch.E. J.* **22**, 417.

Krieger, I. M. 1972 *Adv. Colloid Interface Sci.* **3**, 111.

Krieger, I. M. & Equiluz, M. 1976 *Trans. Soc. Rheol.* **20**, 29.

Lodge, A. S. & Wu, Y. 1971 *Rheol. Acta* **10**, 539.

RUSSEL, W. B. 1976 *J. Colloid Interface Sci.* **55**, 590.
SAVILLE, D. A. 1977 *Ann. Rev. Fluid Mech.* **9**, 321.
SMOLUCHOWSKI, M. V. 1917 *Z. Phys. Chem.* (*Leipzig*) **92**, 129.
SPIELMAN, L. A. 1970 *J. Colloid Interface Sci.* **33**, 562.
STONE-MASUI, J. & WATILLON, A. 1968 *J. Colloid Interface Sci.* **28**, 187.
STONE-MASUI, J. & WATILLON, A. 1975 *J. Colloid Interface Sci.* **52**, 479.
VERWEY, E. J. W. & OVERBEEK, J. TH. G. 1948 *The Theory of the Stability of Lyophobic Colloids*. Elsevier.